Mars Exploration Rover Heatshield Observation Campaign

Christine E. Szalai[1], Benjamin L. Thoma[2], Wayne J. Lee[3], Dr. Justin N. Maki[4]
Jet Propulsion Laboratory, California Institute of Technology, Pasadena, CA, 91109

William H. Willcockson[5]
Lockheed Martin Space Systems Company, Denver, CO, 80201

Dr. Ethiraj Venkatapathy[6]
NASA Ames Research Center, Moffett Field, CA, 94035

and

Todd R. White[7]
ERC, Inc., NASA Ames Research Center, Moffett Field, CA, 94035

For the first time ever, engineers were able to observe a heatshield on the surface of another planet after a successful entry through the atmosphere. A three-week heatshield observation campaign was conducted in December 2004 after the Mars Exploration Rover *Opportunity* exited "Endurance Crater." By utilizing the rover's scientific instruments, data was collected to make a qualitative assessment of the performance of the heatshield. This data was gathered to gain a better understanding of how the heatshield performed during entry through the Martian atmosphere. In addition, this unprecedented look at the heatshield offered engineers the opportunity to assess if any unexpected anomalies occurred. Once a survey of the heatshield debris was completed, multiple targets of interest were chosen for the collection of imaging data. This data was then used to assess the char depth of the thermal protection material, which compared well with design and post-flight computational predictions. Extensive imaging data was collected and showed the main seal in pristine conditions, and no observable indications of structure overheating. Additionally, unexpected vehicle dynamics during the atmospheric entry were explained by the observation of thermal blanket remnants attached to the heatshield.

Nomenclature

α_T	=	total angle of attack
CH	=	film coefficient
ρ	=	density
ε	=	emissivity
Φ	=	non-dimensional material density ratio
q	=	surface heating rate

[1] Senior Systems Engineer, EDL Systems and Advanced Technologies, M/S 301-490, non-member.
[2] Senior Mechanical Engineer, Spacecraft Mechanical Engineering Section, M/S 179-225L, non-member.
[3] Principal Member of the Technical Staff, Systems Engineering Section, M/S 321-467, non-member.
[4] Senior Engineer, Instrument Systems Implementation and Concepts, M/S 321-220, non-member.
[5] Senior Staff Engineer, Entry Systems, Sensing & Exploration Systems, M/S 8003, non-member.
[6] Chief Technologist, Entry Systems and Technology Division, M/S 229-3, Associate Fellow.
[7] Research Scientist, Reacting Flow Environments Branch, M/S 230-2, AIAA member.

I. Introduction

THE Mars Exploration Rover (MER) mission successfully landed two rovers on the surface of Mars. The first, named *Spirit*, landed near Gusev Crater on January 3, 2004 (PST) and the second, named *Opportunity*, landed on Meridiani Planum on January 24, 2004 (PST). The goal of the identical rovers was to learn about ancient water and climate on Mars. Led by principal investigator, Dr. Steve Squyres, professor of astronomy at Cornell University, discoveries made by the MER mission were chosen by *Science* magazine as "Breakthrough of the Year" in its December 17, 2004 edition. This top honor was awarded for the mission's discovery of evidence of salty, acidic water on the planet's surface that may have been hospitable to sustaining life. Originally slated for a primary mission of 90 sols (or Martian days), the two rovers far exceeded expectations, and *Opportunity* is now well past 2500 sols of successful operation, and still going strong. *Spirit's* mission recently ended after unsuccessful attempts to reawaken the rover after a stressful Martian winter.

Both MER landers utilized direct entry into the Martian atmosphere and decelerated through the use of an ablative heatshield, a parachute, and rockets. Figure 1 shows the entry, descent, and landing (EDL) timeline for the mission.[1] The MER mission leveraged off of the successful Mars Pathfinder landing system by utilizing a bridle descent from the entry vehicle and air bags to protect the rover upon surface impact. As shown in Figure 2, the entry vehicle forebody, like Viking and Mars Pathfinder before it, was a 70 degree half-angle sphere cone, with a diameter of 2.65 m. The entry aeroshell, designed and built by Lockheed Martin Space Systems Company, consisted of an aluminum honeycomb composite structure heatshield and backshell assembly with an ablative Thermal Protection System (TPS). The heatshield and backshell were held together by six retention and release mechanisms, which were activated by frangible nuts and springs. Figure 3 shows the entry vehicle mated to the cruise stage with half of the external thermal blanket installed.

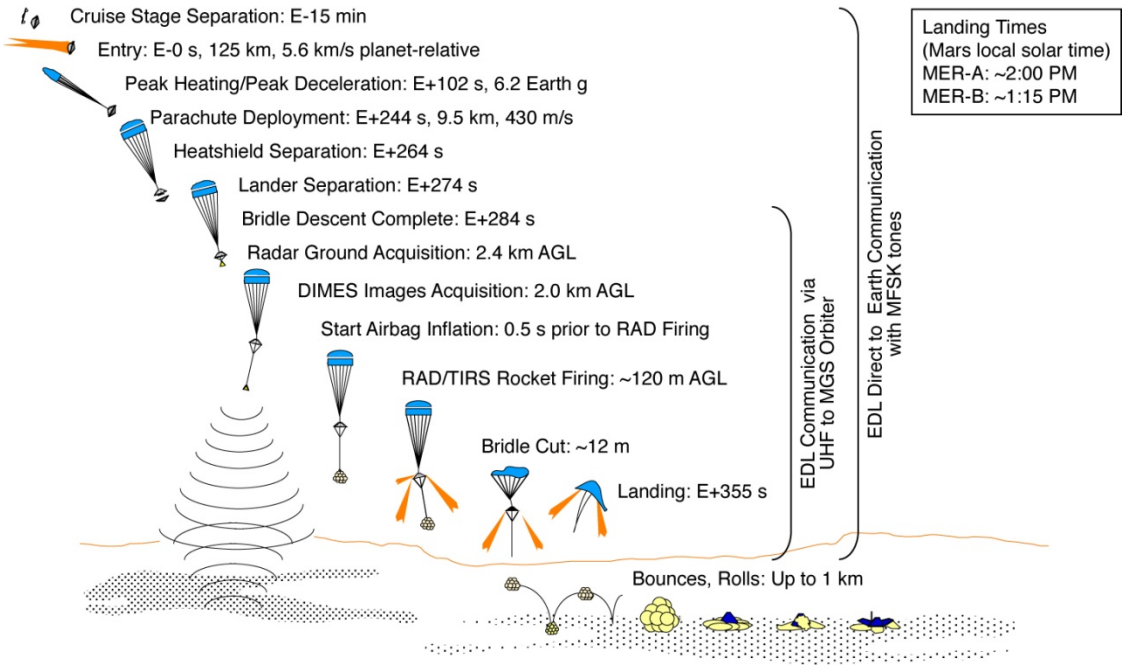

Figure 1. MER Entry, Descent, and Landing Timeline (MER-A, *Spirit*; MER-B, *Opportunity*)

Successful entry into the Martian atmosphere relies on the TPS to protect the rover, inside the entry vehicle, from the harsh heating environment experienced during atmospheric entry. The heatshield TPS utilized on MER was SLA-561V, a Lockheed Martin ablative material that was used on the Viking and Mars Pathfinder missions. The SLA-561V material is composed of phenolic honeycomb cells that are packed with organic compounds and fillers. The material is designed to ablate as a heat rejection mechanism, as shown in Figure 4. An ablative material contains organic resins, which through an endothermic process, decompose (or pyrolyze) and escape from the material surface in the form of pyrolysis gases that then thickens the boundary layer. In addition, carbonaceous products from the decomposition process deposit on the material surface to create a char layer with a high emissivity, which re-radiates back into the boundary layer. The net heat flux is then conducted through the material thickness to the spacecraft structure.

The heatshield TPS thickness is designed to ensure adequate thermal protection of the structure so that the structure maintains its mechanical integrity throughout EDL. A computational thermal model of the TPS is used to predict the material thermal response to the entry environment. These computational models are anchored to data from arc jet testing of the material, but uncertainties still exist. For example, arc jet tests are conducted in air and extrapolated to carbon dioxide as opposed to testing in carbon dioxide, of which the Martian atmosphere is composed. Typically, margin and factors of safety are added to TPS thickness designs to account for any "unknowns" that may occur during the actual Martian entry. Very little flight test data exists for Martian entries and thus there has been little basis for reducing these material design margins from mission to mission. Although entry instrumentation was flown on the Mars Pathfinder heatshield, the combination of the limited number of sensors and the failure of the strategic stagnation point thermocouple produced little or no improvement in computational predictive capability.[2]

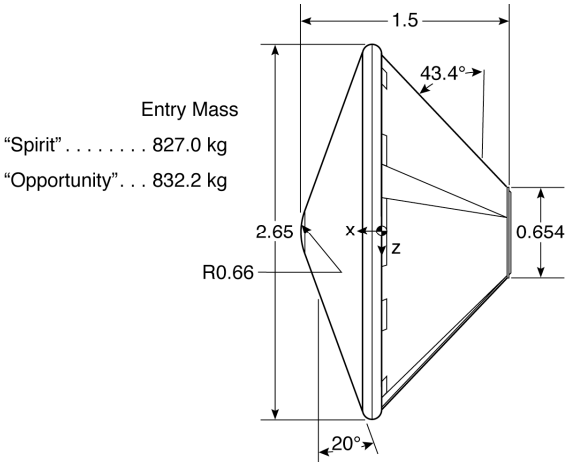

Figure 2. MER Entry Vehicle Configuration (dimensions in meters)

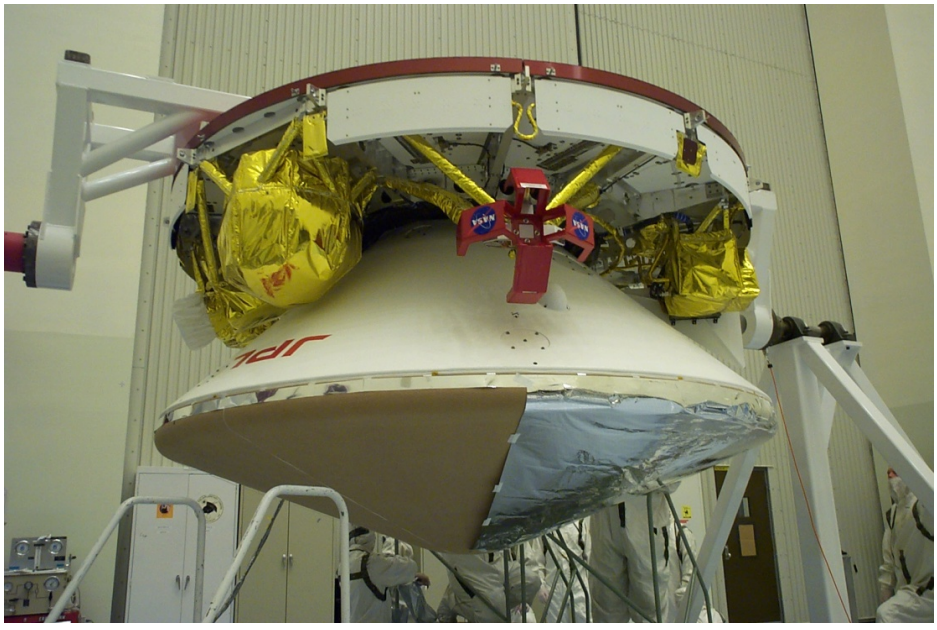

Figure 3. MER spacecraft mated to cruise stage (half of external thermal blanket installed)

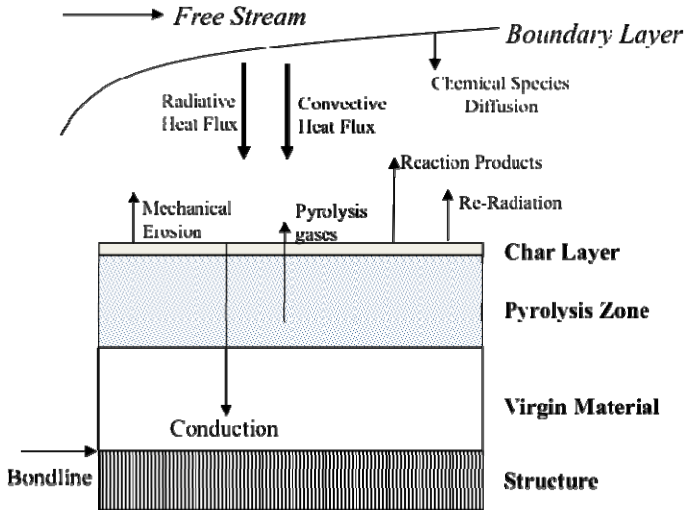

Figure 4. The ablation process of a thermal protection material

Once the MER heatshield successfully performed its function of protecting the spacecraft structure and providing over 90% of the entry velocity reduction, the parachute was deployed and shortly afterwards the heatshield was jettisoned to allow subsequent rover deployment. The expended heatshield then fell to the surface with an estimated impact speed of 76 m/s (170 mph). For *Opportunity*, this uncontrolled descent resulted in the heatshield impacting 820 m east-southeast of the rover's initial landing site, on a flat plain south of Endurance Crater. This location was observed by the rover shortly after its successful landing, and was subsequently confirmed by the orbiting Mars Global Surveyor spacecraft. After landing, the *Opportunity* rover spent time exploring and analyzing the unique bedrock outcrop nearby and entered "Endurance" crater in June 2004.

In early December 2004, once the *Opportunity* rover exited "Endurance" crater, engineers were given the unique opportunity to utilize the rover to observe the heatshield on the surface of Mars. There was no instrumentation on the MER heatshield to provide data on its performance, and this opportunity offered an unprecedented look at a heatshield after a Mars entry. There were several instruments on-board the rover that could be utilized to gain useful information regarding the performance of the heatshield and this data then has the potential to impact future heatshield designs.

II. *Opportunity* Rover Assets

The MER rovers have high-resolution cameras and a Microscopic Imager (MI) that were used for this observation campaign. Two Navigation Cameras (Navcams) and four Hazard Avoidance Cameras (Hazcams) were primarily used for traverse planning and rover fine positioning for the Instrument Deployment Device (IDD). The Navcams are mounted on the rover 1.54 m above the Martian surface and have an optimum best focus depth of field of 1.0 m. The Navcams can provide 360° panoramas, as well as stereo and monoscopic images. The Hazcams are mounted on the rover 0.5 m from the surface and are specified to provide about 15° of sky in the top portion of the images. The Hazcams have a best focus depth of field of 0.5 m.[3]

The Panoramic Camera (Pancam) is a high resolution, color, stereo panoramic imaging system consisting of two

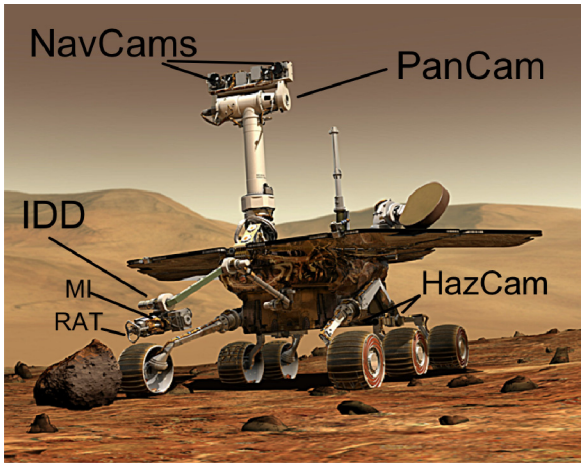

Figure 5. Mars Exploration Rover and Science Assets

digital cameras mounted on a mast 1.5 m above the Martian surface. The mast allows a full 360° image in azimuth and ±90° in elevation. The Pancam was designed and optimized to assess the high-resolution morphology, topography, and geologic context of each MER landing site.[4] For the heatshield observation campaign, the Pancam provided high-resolution (~1 mm/pixel at a range of 3 m from the rover) color images of the hardware and debris field.

The rover's science payload includes a five degree of freedom IDD arm that carries four tools: the MI, an Alpha Particle X-ray Spectrometer (APXS) for elemental chemistry, a Mössbauer Spectrometer (MB) for the mineralogy of iron-bearing materials, and a Rock Abrasion Tool (RAT) for removing dusty surfaces and exposing fresh rock underneath.[5] The RAT and the MI were considered for use in the observation campaign. The MI could be used for close-up magnification (fixed at 0.4) of the heatshield surface and the RAT could be used to remove a certain depth of material to obtain images of the material char layer. Laboratory tests were conducted with an engineering RAT unit and a charred SLA-561V material sample to evaluate if this tool could be used on the heatshield. Test results showed that the RAT abrasion process on the char surface layer produced a large amount of carbon dust that then prevented an assessment of char layer depth within the resultant cross-section. This char dust also contaminated the engineering RAT and thus was unacceptable for *Opportunity*'s RAT since it may cross-contaminate future science investigations on Martian rocks. Thus it was decided that the RAT would not be used for the heatshield observation campaign. The MI could still be utilized, however, as long as the MI surface did not come in contact with the heatshield. The rover and location of these science assets are shown in Figure 5.

III. Heatshield Observation Plan

A team was formed from MER team members at JPL, Lockheed-Martin, and NASA Ames Research Center, and included engineers familiar with the TPS design and spacecraft hardware. This team created a prioritized investigation plan that the MER Operations team would implement:

1) Obtain imaging data to determine char depth of localized area of material. This information can be used to directly compare TPS performance vs. computational predictions.
2) Obtain imaging data to look at global charring patterns on heatshield. Surface color variability and surface feature observations (e.g. surface roughness) can allow a qualitative comparison to Computational Fluid Dynamics (CFD) aerothermal heating prediction trends and ground test results.
3) Obtain imaging data to evaluate the performance of the main thermal seal. This main thermal seal prevented hot gas ingestion into the spacecraft during entry at the interface between the heatshield and the backshell. Imaging data can be used to assess the integrity of the seal and evaluate if any burn-through occurred.
4) Obtain imaging data of the internal structure. Observation of structure color variability may indicate thermal gradients and structure over-heating, if it occurred.

In addition, visible evidence of a cause for the unusual entry oscillations, observed late in both entry vehicle's hypersonic and supersonic flight phases, was sought as a target of opportunity. In order to begin the observation campaign, a comprehensive imaging survey of all heatshield debris was planned. In addition to assisting in the determination of targets of interest, this information could be used to evaluate if any anomalies occurred.

IV. Observation Results

Once *Opportunity* exited "Endurance" crater in December 2004, the rover began driving towards the heatshield. Figure 6 shows a PanCam image of the heatshield taken on Sol 322 as the rover was about 130 m away. At this point, it was clear that the heatshield was not intact after impacting the surface at about 75 m/s (170 mph). Although the heatshield's free-fall descent was expected to be generally stable, the flight dynamics of such a shallow dish could still result in a large range of impact attitudes.

It was hoped that impact occurred at an angle that would preserve significant portions of the fragile TPS. However, as the rover approached, it became apparent that the conical heatshield had impacted nearly vertically, as witnessed by the circular symmetric shape of the impact divot, as shown in Figure 7. It appears that the western edge of the divot may have been the initial impact point, so the angle of attack could have been as much as 30-40 degrees. This event had the effect of breaking the nose loose and driving it through the structure to a fair distance away. As the rest of the conical structure drove itself into the soil, it broke apart along the pie-shaped manufacturing splice joints, flattening onto the surface, and resulting in most of the external surface impacting with a fair amount of energy. This was unfortunate in that it caused most of the exterior TPS to impact the ground, breaking up the

relatively fragile outer char layer that contained evidence of flow-lines. This had the effect of scrubbing off the char layer, but it left behind the un-charred (virgin) TPS. Thus the remaining TPS represented a reasonable demarcation between charred and un-charred zones.

As the impact process continued, the broken heatshield petals rebounded from the initial impact, and came to rest in two major groups roughly 10 m to the northeast. The largest group actually landed inverted with the TPS surface largely hidden. As shown in Figures 6 and 7, this process exposed the shiny, reflective internal multilayer insulation (MLI) blankets, which were integrated to the inside of the heatshield. Figure 8 shows the debris field when the rover was about 30 m away from the heatshield. These images obtained by the rover provided the information needed to implement the prioritized investigation plan.

It was hoped that the stagnation point, or "nose", of the heatshield, which corresponds to the highest heating location on the heatshield, was located at the secondary debris site, named the "flank" piece. Since this is a critical location on the heatshield, the plan was to drive the rover to the "flank" piece first and obtain imaging data. The MI would then be used to obtain char depth information, if a target of acceptable quality was identified. After the flank piece was evaluated, the plan was then to survey the main heatshield debris by circling around to obtain imaging from each main direction. The rover would then drive in close to the exposed seal location to obtain imaging of the seal and internal structure. If a worthy target was identified on the main heatshield piece, the MI would be utilized to gather char depth information from the resulting images.

Figure 6. Heatshield Debris Image from Sol 322 (Rover approximately 130 m away)

Figure 7. Main heatshield, "flank piece", and impact divot

Figure 8. Images of the heatshield debris field taken from a 30 m distance (impact divot on right)

A. The "Flank" Piece

Sol 329 and 330 imaging of the "flank" piece provided a survey of the broken heatshield and structure at this location, and Figure 9 identifies these pieces. Circling around the flank piece gave intriguing vantage points and color images of the debris by utilizing the PanCam (shown in Figures 10 and 11). MI data was obtained on a couple of areas, including the stagnation transition piece, as seen in Figures 12 and 13. At the stagnation transition piece, the IDD was not able to position the MI to obtain a true cross-sectional view of the exposed edge. Therefore char depth could not be evaluated at this location on the heatshield. Good aerial views of the TPS surface were obtained (Figures 10-13) which were hoped to show global charring patterns (investigation objective 2), however the impact destruction of the fragile TPS char surface had eliminated any such patterns. The "flank" structural remnants did confirm the heatshield thermal integrity for this portion of the heatshield. The exposed main seal and aluminum honeycomb were all in pristine condition, showing only impact damage and no signs of hot gas ingestion, thermal distress, or discoloration. Since the "flank" piece debris did not offer areas where char depth evaluation could easily be obtained, it was decided to traverse to the main heatshield.

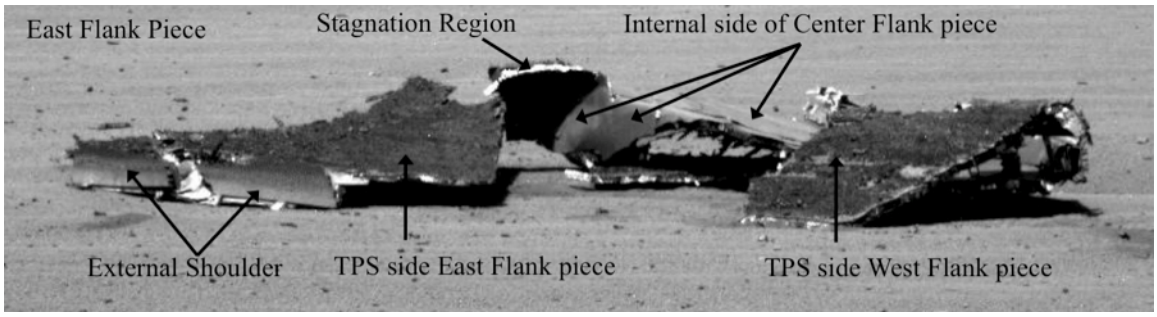

Figure 9. Identification of the "flank" pieces

Figure 10. Sol 331 image of "flank" piece from the South (the rover's solar panels can be seen in the foreground)

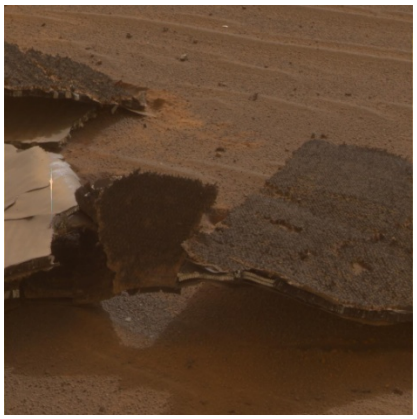

Figure 11. Color PanCam image of the heatshield stagnation area

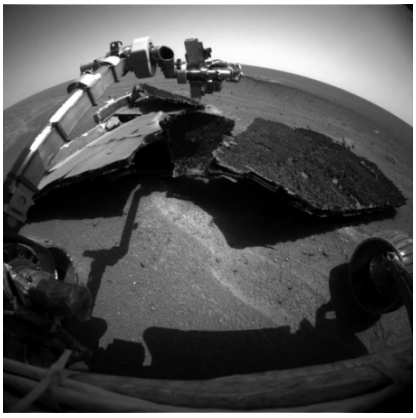

Figure 12. *Opportunity*'s Instrument Deployment Device positioning the MI for close-up images

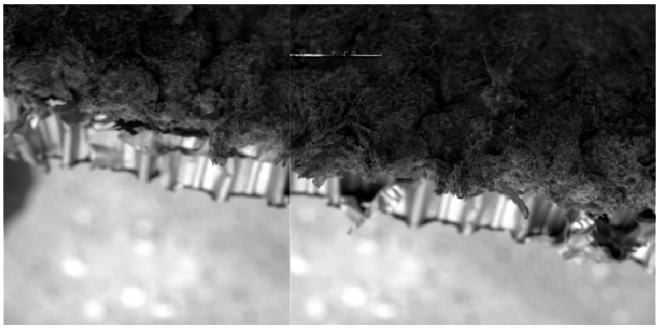

Figure 13. MI images of the "flank" piece stagnation area

B. The Main Heatshield

Before it was determined that the heatshield was inverted, it was hoped that observation of the global charring pattern on the exterior surface of the TPS would offer insight into heating gradients and transition to turbulence. Images were taken from various angles around the main heatshield, and at different times of the Martian day, to attempt to distinguish color patterns on the TPS. Unfortunately because the inverted position shadowed and blocked the interior, clear images of the TPS could not be obtained, as seen in Figure 14. However, this side of the main heatshield offered excellent cross section targets to obtain char depth measurements.

The heatshield shoulder is shown in Figure 15 and a close-up is shown in Figure 16, which also shows the MI target of the "flank" region cross-section. Figure 17 shows the mosaic MI results at this "flank" cross-section and shows significant impact damage to the TPS. Assuming the char layer has been removed, the remaining virgin material is estimated at a depth of 10.2 mm. A comparison to predictions is described later in the Analysis section. The "edge" location at the shoulder, as

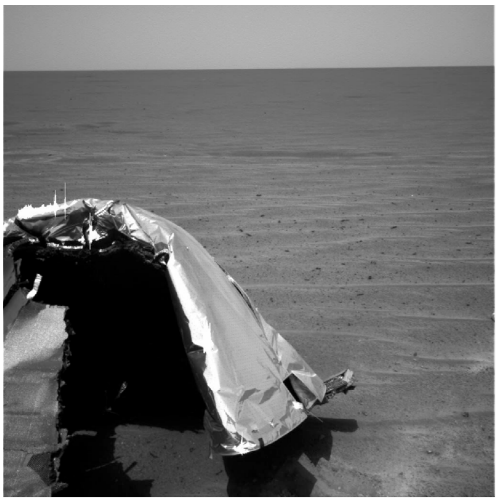

Figure 14. Main heatshield image in the attempt to view TPS surface characteristics

shown in Figure 18, turned out to be an excellent cross sectional view, and the MI results are shown in Figure 19. An estimate of the char depth, based on slight color variations, was made (3.3 mm) and a comparison to char thickness predictions is discussed in a later section. This data allowed engineers to achieve one of the main objectives of the heatshield observation plan. An interesting view and color image of the shoulder area is shown in Figure 20. The mottled appearance is likely due to heating gradient effects on the TPS at the shoulder region.

Figure 21 shows the internal MLI blanketing, a separation spring, and fortuitously, a rock that intrigued the MER scientists. A color image from Sol 357 (Figure 22) revealed the heatshield composite structure, fractured and rippled from the high-speed impact into the Martian surface. These color images showed no observable discolorations on the structure or internal MLI blanketing that would indicate overheating. Many of these elements are quite thin, and thus very susceptible to thermal damage, particularly the aluminum honeycomb and MLI, so these visual results are quite conclusive. This result achieved the fourth main objective of the observation plan.

This vantage point and the same color image also show that the main seal appeared to be in pristine condition, with no observable sign of hot gas penetration through the seal. There were also no observable discolorations that would indicate overheating, and this observation achieved the third main objective of the observation. Further images taken on Sol 357 proved to be some of the most valuable images of the entire observation campaign.

Figure 15. Sol 329 image of the main heatshield from the west

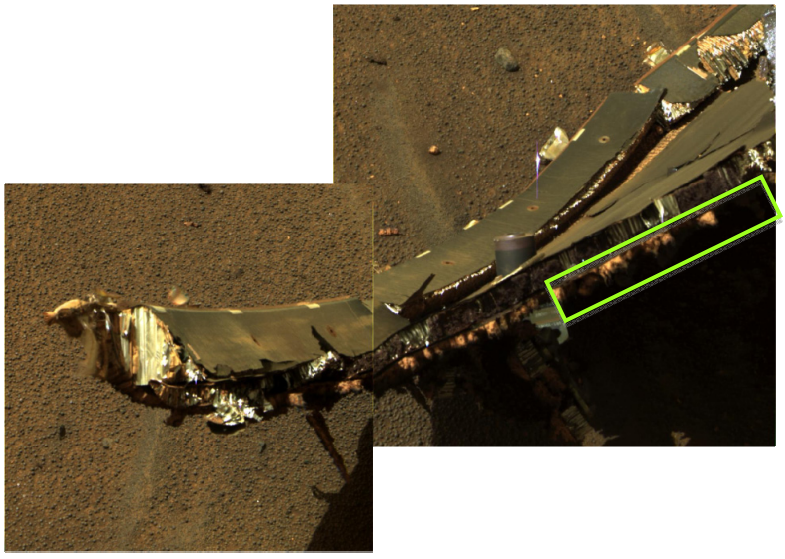

Figure 16. Mosaic close-up image of the heatshield shoulder and MI target for "flank" region (heatshield rim is to the left and TPS is facing down)

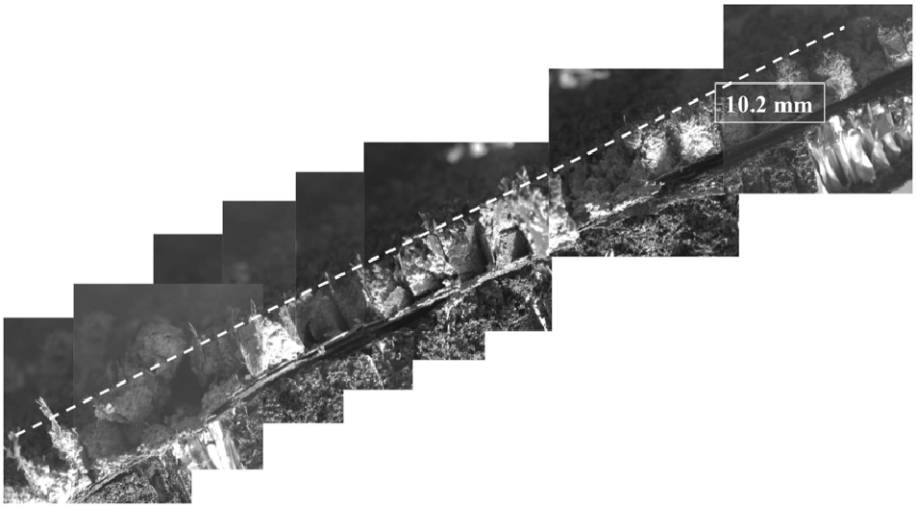

Figure 17. Mosaic of "flank" region MI with estimated virgin layer remaining

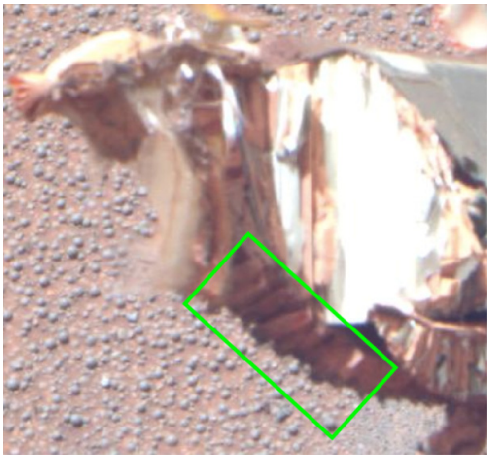

Figure 18: MI target area at heatshield edge

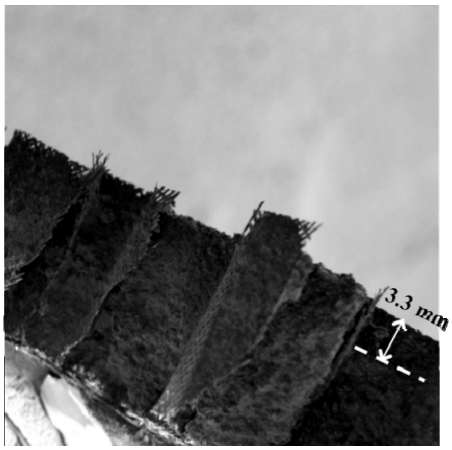

Figure 19. MI image of heatshield edge with estimated char layer depth

Figure 20. Color image of heatshield shoulder

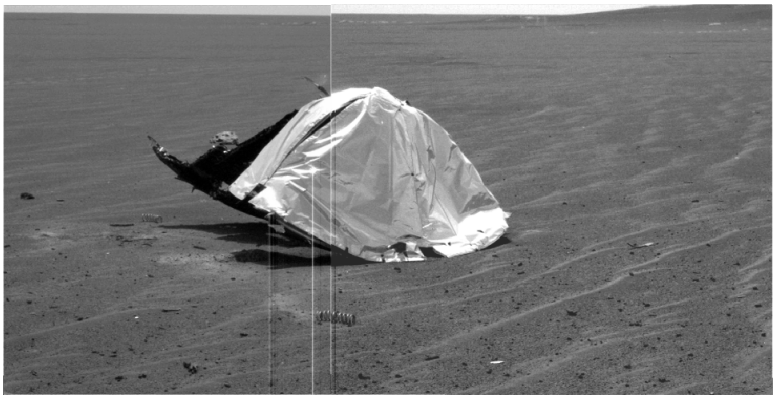

Figure 21. Sol 335 image of the heatshield ("heatshield rock" can be seen just behind the heatshield)

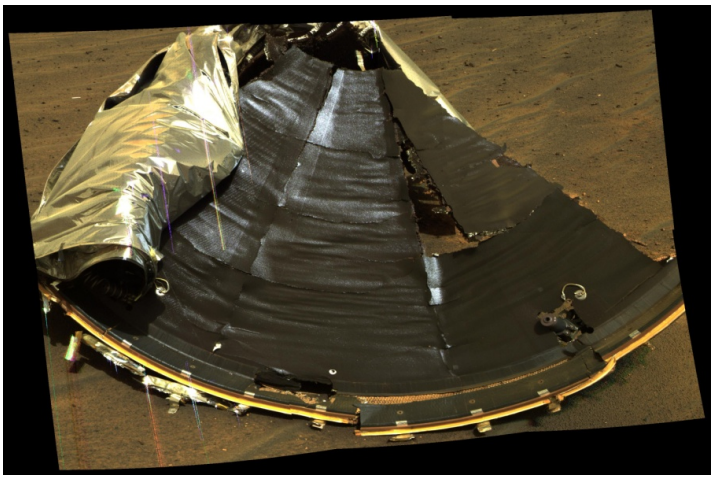

Figure 22. Heatshield structure and main seal

C. A Major Discovery – External MLI Blanket Remnants

Figure 23 shows a close-up of the main seal area, and clearly shows remnants of the aluminized mylar tape interface and thermal blanket "keeper strips" that were used to attach the external MLI blanket to the heatshield. This external MLI blanket was needed for thermal control of the spacecraft during cruise. The observation of these remnants led engineers to explore the possibility that this may be an explanation for a mystery that had plagued the MER flight reconstruction efforts.

Figure 24 shows the entry attitude reconstruction for *Opportunity*. This plot shows angle of attack oscillations much earlier, and at magnitudes far in excess of what was expected. Similar anomalous behavior was also observed during *Spirit*'s entry three weeks earlier. This behavior was not seen in the post-flight reconstruction of the Mars Pathfinder spacecraft. Thus this unexplained behavior was causing consternation for design engineers who were designing the EDL system for the next Mars mission at

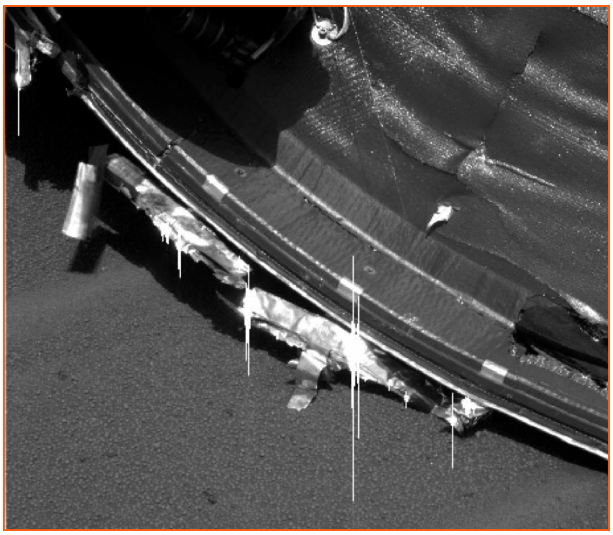

Figure 23. Thermal blanket "keeper strips" and tape interface for external thermal blanket remnants

the time, Phoenix. Aerodynamicists studied the effect that this tape strip could have had on the entry dynamics. This work is detailed in Reference 6, and it was concluded that this tape strip remnant, acting as an aerodynamic "scoop", could have been enough of a disturbance in the flow field to explain the anomalous angle of attack oscillations during entry. This discovery has thus drawn attention to the design of external MLI blanket attachment schemes for future Mars missions. Fortunately, the Phoenix spacecraft did not need an external thermal blanket for thermal control during the cruise phase. It is now clear that the blanket attachment design must avoid aerodynamic trapping geometries that will block flow. This may be accomplished via complete burn-off during atmospheric entry, or mechanical removal, of the blanket and any continuous attachment strips to avoid any possible flow field disturbance that would adversely affect entry dynamics. Streamers of material are not much of a problem since they will rapidly disintegrate in the high-energy flow with little long-term effect. Careful attention, however, must be paid to remnant materials on the lee-side of the entry body since they can be protected during the primary heat pulse and then later be exposed as the wake narrows with lower velocities. Such was the case with both MER entry vehicles.

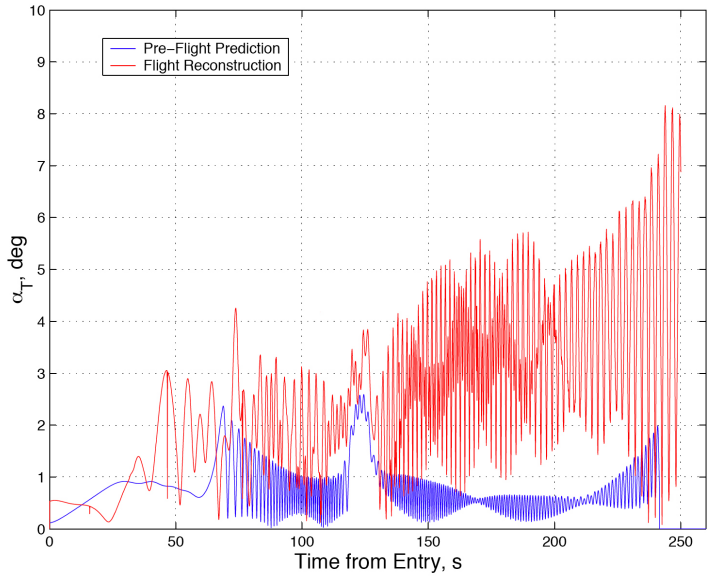

Figure 24. *Opportunity* entry attitude reconstruction (from Reference 6)

D. "Heatshield Rock"

Opportunity's heatshield fortuitously landed near a unique, basketball-sized rock (Figure 25), aptly named "heatshield rock" by MER scientists. During the heatshield observation campaign, the scientists took a detour around the heatshield to gather spectroscopic data on the rock to aid in its identification. Surprisingly, it was determined to be an iron-rich meteorite, and the first meteorite of any type ever to be identified on another planet. This unexpected science "gem" could open up research possibilities for future robotic and sample return missions.

Figure 25. "Heatshield Rock", the first ever meteorite identified on another planet

V. Analysis

The original design analysis for the MER entry vehicle TPS sizing was conducted by Lockheed Martin, using the Langley Aerothermodynamic Upwind Relaxation Algorithm (LAURA) code for CFD-based aerothermal

predictions, and the Reacting Kinetic Ablation Program (REKAP) code for SLA-561V TPS material response. NASA Ames Research Center performed independent verification and validation of this analysis utilizing the General Aerodynamic Simulation Program (GASP) CFD code and the Fully Implicit Ablation and Thermal response (FIAT) code for TPS material response. The availability of the best-estimated trajectory (BET), and identifiable regions of the MER heatshield motivated a post-flight aerothermal and material response activity at NASA Ames Research Center using analysis tools and models developed since MER. The MER-B (*Opportunity*) BET is defined starting at entry interface (EI) at an altitude of 125 km with velocity 5.4 km/s and continues until heatshield separation some 300 seconds later (Figure 26). The time-varying atmospheric density and temperature, along with velocity are the boundary conditions to the hypersonic computational flow solver.

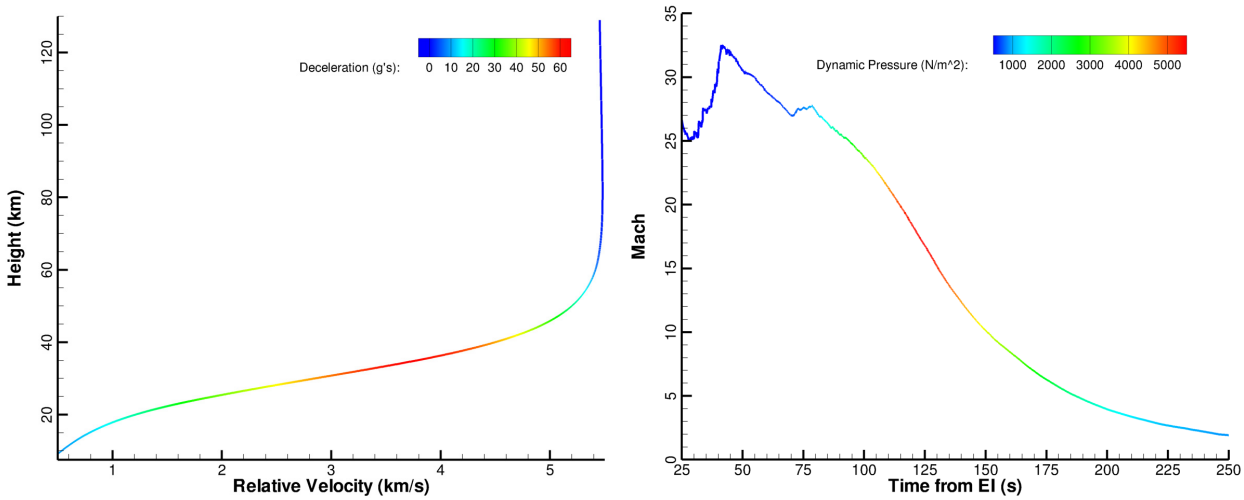

Figure 26. *Opportunity* reconstructed entry profile

A. Aerothermal Environments

The MER-B heatshield is simulated as a series of steady-state flows with the Data Parallel Line Relaxation (DPLR) code v4-02-1. DPLR is a modern, parallel, structured non-equilibrium Navier-Stokes flow solver maintained at NASA Ames Research Center.[7] The code employs modified Steger-Warming flux-splitting scheme, for higher-order differencing of the inviscid fluxes, and is run here with 2nd spatial accuracy and to steady-state 1st order in time. DPLR has been validated over a wide spectrum of flight and ground-based experimental simulations. For the following analysis, the 2-D/axisymmetric version of DPLR is used, with a grid of 100 points in both the surface and surface-normal directions.

The flow around MER-B's heatshield is modeled as turbulent thermochemical non-equilibrium flow, using the Mitcheltree and Gnoffo 8 species 12 reactions Mars atmosphere (CO_2, CO, N_2, O_2, NO, C, N, O).[8] For the current analysis, the angle-of-attack is held constant at 0 degrees, and a series of steady-state axisymmetric flow-field simulations are performed at 21 discrete times throughout the trajectory. The TPS surface is modeled as non-slip radiative equilibrium wall with constant emissivity ($\varepsilon = 0.85$) and Mitcheltree and Gnoffo surface catalycity model.[8] Menter's shear stress transport (SST) vorticity-based turbulence model with Wilcox blended compressibility correction[9] is used, with a turbulent Schmidt number of 0.7. Due to the small vehicle diameter and low entry velocity, radiative surface heating is negligible and is omitted.

The convective heating reaches a peak of 44 W/cm^2 (Figure 27) at the stagnation point after 95 seconds from entry interface, and is consistent with MER heat shield design environments.[10,11] The steady-state CFD predicted surface pressure, film-coefficient, and recovery enthalpy are fitted in time, and provided as boundary conditions for the TPS material response simulations. Representative environments for the stagnation point, mid-flank, and edge are shown in Figures 27-29. The area around the stagnation point remains laminar, and has the overall highest heating, while the flank and edge points both experience transition to turbulent heating at around 80-90 seconds after entry interface.

B. Material Response Simulations

Along the heat shield, a series of surface-normal material response calculations are performed using FIAT v2.5.1.[12] FIAT computes the transient 1-D thermal response to an aerothermal heating profile for a material stack-up including thermal protection, bonding, and structural materials, in this case, for SLA-561V and the specific substructure beneath the MER-B heatshield.

For this analysis, a FIAT simulation is performed at each CFD grid point. In the past, such extensive 1-D or limited 2-D TPS analysis would not be performed, but was necessary here given uncertainty in location of images relative to the as-built geometry. The FIAT 1-D grids and results are then unwrapped and rotated back into the CFD coordinate system for comparison with imagery. A detail of the heatshield shoulder with the shock-tailored[13] DPLR grid and FIAT material grid is shown in Figure 30.

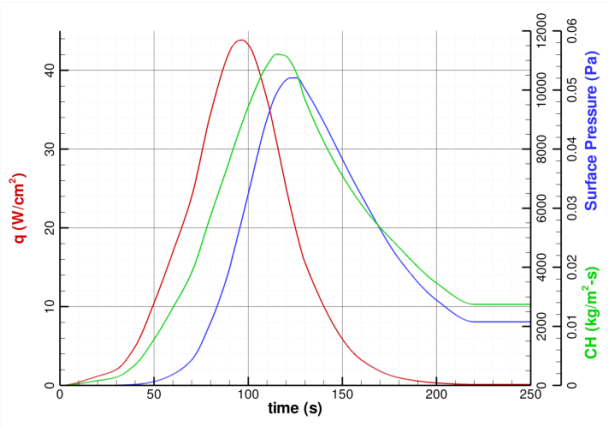

Figure 27. Stagnation point environment from DPLR

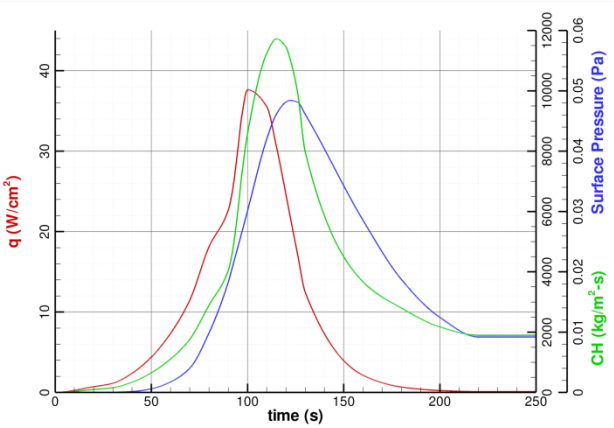

Figure 28. Mid-flank environment from DPLR

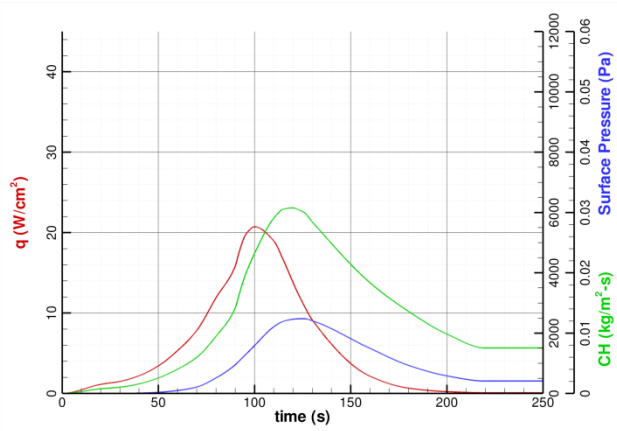

Figure 29. Edge environment from DPLR

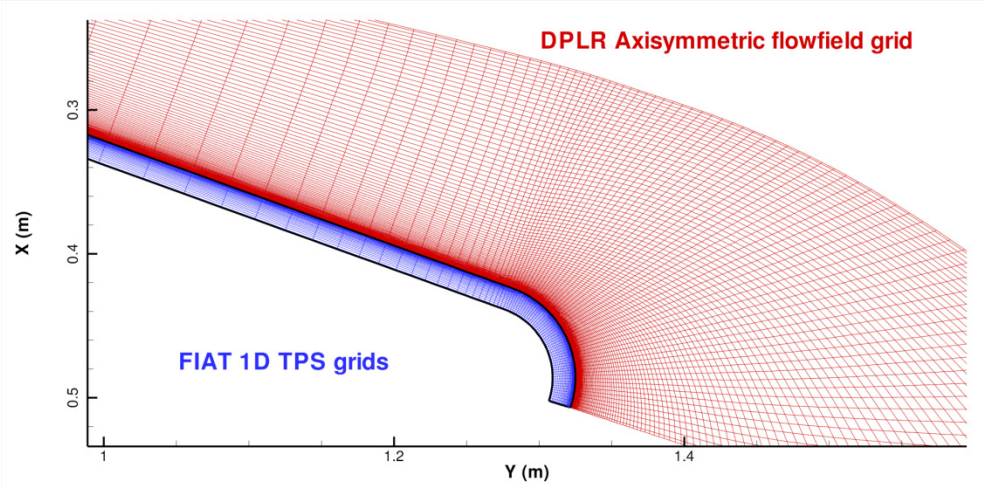

Figure 30. Detail of computational grids for DPLR and FIAT

For the TPS material response, the SLA-561V High Fidelity Response Model developed during the Mars Science Laboratory (MSL) program is used.[14] Each 1-D stack-up starts with a uniform temperature of 200 K, and after 250 seconds, a cool-down period allowing radiant cooling to a Mars average surface temperature of 250 K. At the completion of the cool-down period, the final through-the-thickness density profile of the TPS is extracted. This density profile is non-dimensionalized as Φ where $\Phi = 0$ is fully charred material, and for $\Phi = 1$ the material is fully virgin, according to:

$$\Phi = \frac{(\rho - \rho_{char})}{(\rho_{virgin} - \rho_{char})}$$

Figure 31 shows the FIAT predicted density profile for a slice through the entire heat shield. The boxed Flank and Edge regions encompass two of the zones with MI images. The size of the box indicates the uncertainty in the exact location of these images relative to the as-built heat shield.

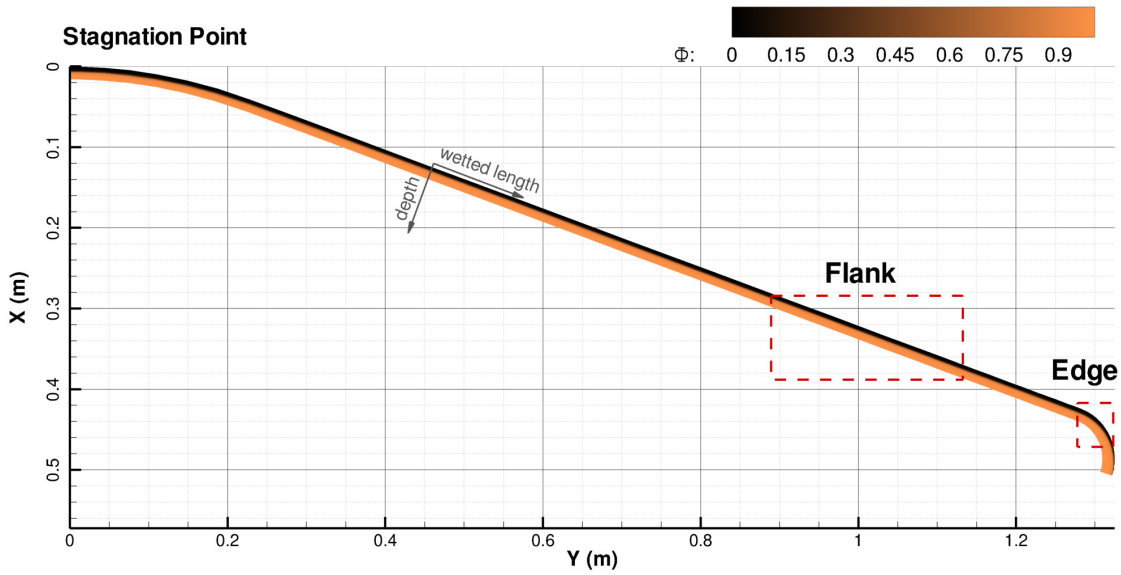

Figure 31. DPLR and FIAT predicted TPS density profile and regions for comparison

C. Comparison of Analysis with Imagery Measurements

As expected, there is no measurable surface recession as SLA-561V performs mainly as a charring insulator. The Flank location is much more uniform in profile than the Edge section, which experiences varied environments due to the shoulder curvature. The two regions highlighted in Figure 31 (Flank and Edge) and imaged in Figures 17 and 19, are shown in greater detail in Figures 32-33 below. Here, the TPS is plotted as depth (measured from the TPS outer-mold line) vs. wetted length (measured from the stagnation point). The X and Y coordinates consistent with Figure 31 are also shown. The char thicknesses determined from Figures 17 and 19 are included for comparison.

The precise Φ at which the TPS cross section color shade changes is material dependant, and not well defined for this type of examination of SLA-561V. FIAT uses the following simple definition:

$$\Phi < 0.02\text{: Fully Charred Region}$$
$$0.02 \leq \Phi \leq 0.98\text{: Pyrolysis Region}$$
$$\Phi > 0.98\text{: Virgin Region}$$

Using the above definition, the pyrolysis zone is quite wide (approximately half the installed TPS thickness), which leads to a qualitative rather than quantitative comparison. For both MI images (Figure 17 and Figure 19), the comparison to the pyrolysis zone falls within the analysis predicted region, at 50% mass loss or more from the virgin material.

A similar post-flight analysis was conducted by Lockheed Martin using the same aerothermal CFD and TPS response codes used for the original design (LAURA and REKAP), and produced very similar results to what is presented above. The SLA-561V flank virgin thickness based on the BET was 9.1 mm, very close to the 10.2 mm thickness observation estimation. The edge location was more difficult due to the steep heating gradients, but was estimated at 2.0 mm char via linear interpolation of adjacent points. This result compares well to the estimated 3.3 mm char observed in the images.

Both of the NASA Ames Research Center and Lockheed Martin analysis efforts show results that agree reasonably well with the observed state of the TPS on the surface of Mars, providing a basic confirmation of the combined aerothermal and TPS response codes for Martian entry.

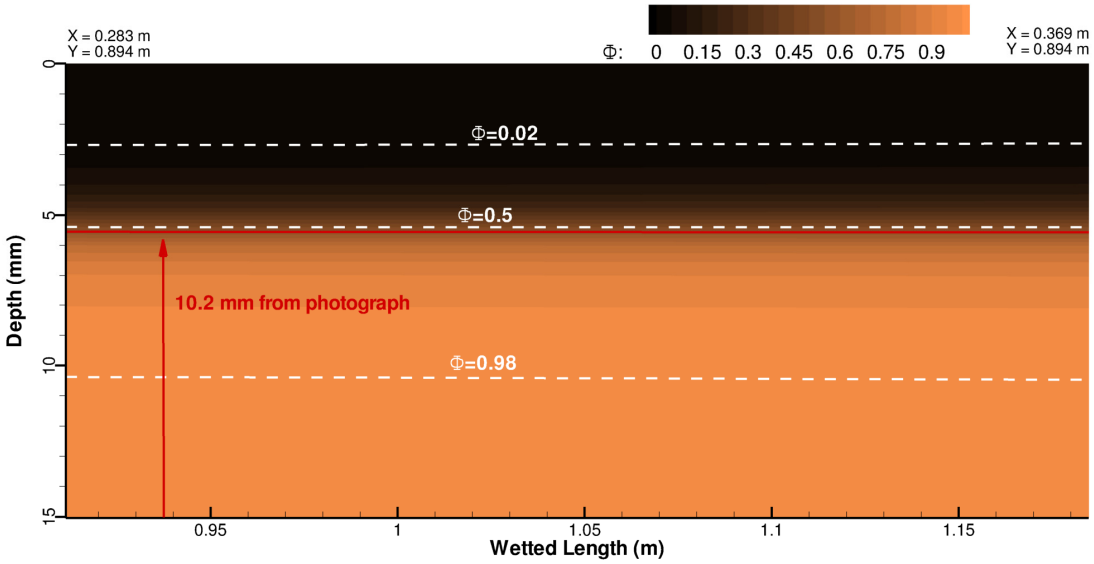

Figure 32. DPLR and FIAT predicted Flank TPS density profile compared with observed

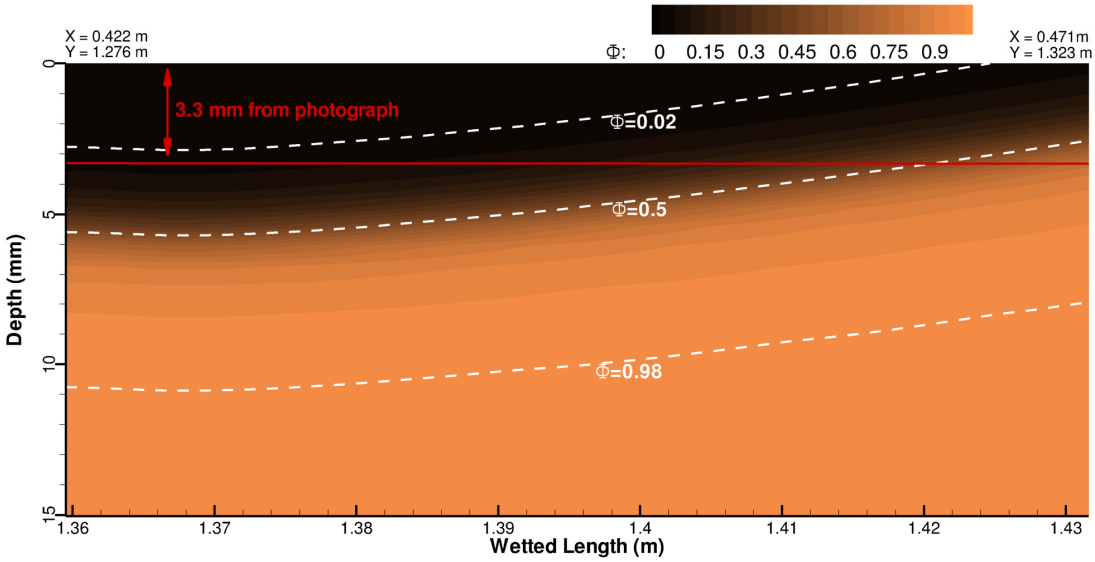

Figure 33. DPLR and FIAT predicted Edge TPS density profile compared with observed

D. Future Analysis

There is the opportunity for forward work to improve comparisons with the MI and other photographs (namely Figures 16, 18, and 20). Additionally, material studies of MSL test-era SLA-561V charred and virgin samples, such as Thermo-Gravimetric Analysis, may provide better mapping of TPS cross-section coloration to material density. This better density mapping, along with FIAT Monte-Carlo simulations[15] will be used to better define the pyrolysis zone and predicted uncertainty. Future studies will also address angle-of-attack variation and TPS blowing, which should have minor effects on the in-depth material performance.

VI. Conclusions

The observation of a heatshield, post-atmospheric entry on another planet, was an unprecedented opportunity for engineers in the aerothermodynamic and TPS community. Designing an EDL system is challenging, and without TPS instrumentation, there is no information on how well the TPS performed in comparison to predictions, how well engineers were able to predict the aerothermal environment, and the appropriateness of the margin approach used in the TPS design. Without this information, it is difficult to feed-forward improvements to TPS design for future missions.

The ability to visually observe *Opportunity*'s heatshield after atmospheric entry proved extremely valuable in making qualitative assessments with respect to the TPS and main seal performance. This observation campaign successfully met three of the four main objectives:

1) Obtain imaging data to determine char depth of localized area of material. Objective met – MI imaging at the shoulder allowed an assessment of char depth that compared well to design and post-flight predictions.
2) Obtain imaging data to look at global charring patterns on heatshield. Objective not met – Due to the scrubbing of the TPS char layer from impact and the inversion of the main heatshield debris, images could not be obtained that would allow an assessment of global heating patterns.
3) Obtain imaging data to evaluate the performance of the main thermal seal. Objective met – Clear, color images of the main seal show no observable signs of overheating or gas penetration through the seal; seal appears to be in pristine condition and confirms adequacy of the seal design.
4) Obtain imaging data of the internal structure. Objective met – Images of the internal structure, though fractured from impact, show no observable signs of discoloration that would indicate overheating.

The critical discovery of external thermal blanket remnants on the heatshield can directly feed-forward to future mission designs. Aerodynamic analyses have shown that these remnants could have been enough of a disturbance in

the flow field to explain the previously unsolved mystery of unexpected angle of attack oscillations during entry. It is clear that external thermal blanket attachment designs need to be carefully assessed aerodynamically so as not to adversely affect entry dynamics.

This observation campaign was extremely successful in gathering an abundance of visual data to allow qualitative assessments of TPS performance and the main seal design. The data gathered showed a char depth consistent with design and post-flight predictions, and a main seal in pristine condition. In addition, there was no indication of overheating on the structure or internal thermal blankets. The MER scientists also got a bonus in the discovery of the first meteorite ever identified on another planet. Though limited and qualitative, this observation campaign provided a basic confirmation of the combined aerothermal and TPS response codes for Martian entry, and yielded critical results that can feed-forward to future missions.

Acknowledgments

This opportunity would not have been possible without the support and advocacy from Rob Manning, Wayne Lee, Dave Lavery, and Doug McCuistion. The authors are also extremely grateful to the MER science team, especially Dr. Steve Squyres and Dr. Ray Arvidson, for allowing weeks of rover operations dedicated to obtaining this critical data. The authors also wish to thank Dr. Prasun Desai for providing the best-estimated trajectory information. Last, and certainly not least, many thanks go to the incredible MER operations team, who carefully drove *Opportunity* through the challenging debris field, operated the rover in non-standard manners, and obtained all of the incredible images that allowed the accomplishment of the heatshield observation campaign objectives. This campaign was carried out at the Jet Propulsion Laboratory, California Institute of Technology, under a contract with the National Aeronautics and Space Administration, and portions of this work were conducted under contract NNA10DE12C to ERC, Inc.

References

[1]Desai, P.N., Lee, W.J., "Entry, Descent, and Landing Scenario for the Mars Exploration Rover Mission," International Workshop on Planetary Probe Atmospheric Entry and Descent Trajectory Analysis and Sciences, Lisbon, Portugal, October 2003.

[2]Milos, F.S., Chen, Y.K., Congdon, W.M., Thornton, J.M., "Mars Pathfinder Entry Temperature Data, Aerothermal Heating, and Heatshield Material Response," AIAA Paper 98-2681, 1998.

[3]Maki, J.N., et al., "Mars Exploration Rover Engineering Cameras," *J. Geophys. Res.*, *108*(E12), 8071, doi: 10.1029/2003JE002077, 2003.

[4]Bell III. J.F., et al., "Mars Exploration Rover Athena Panoramic Camera (Pancam) Investigation," *J. Geophys. Res.*, *108*(E12), 8063, doi: 10.1029/2003JE002070, 2003.

[5]Squyres, S.W., et al.., "Athena Mars rover science investigation," *J. Geophys. Res.*, *108*(E12), 8062, doi: 10.1029/2003JE002121, 2003.

[6]Tolson, R.H., Willcockson, W.H., Desai, P.N., Thomas, P., "Anomalistic Disturbance Torques During the Entry Phase of the Mars Exploration Rover Missions – A Telemetry and Mars-Surface Investigation," 29th Annual AAS Guidance and Control Conference, AAS 06-087, Breckinridge, CO, February 4-8, 2006.

[7]Wright, M. J., Candler, G. V., and Bose, D., "Data-Parallel Line Relaxation Method of the Navier-Stokes Equations," AIAA Journal, Vol. 36, No. 9, 1998, pp., 1603-1609.

[8]Mitcheltree, R.A. and P.A. Gnoffo, "Wake Flow About a MESUR Mars Entry Vehicle," AIAA 94-1958, June 1994.

[9]Brown, J.L., "Turbulence Model Validation for Hypersonic Flows," AIAA 2002-3308, June 2002.

[10]Willcockson, W., Edquist, T., "Mars Exploration Rover TPS Peer Review: SLA-561V Data and Modeling for Heatshield," May 10, 2001 (unpublished).

[11]Tauber, M., et. al, "ARC Mars 2003 Aerothermal Environment and TPS Sizing Preliminary Studies," NASA Ames Document A9SP-0004-XD001, 2001 (unpublished).

[12]Milos, F.S., Chen, Y.-K. and Squire, T., "Updated Ablation And Thermal Response Program For Spacecraft Heatshield Analysis," Paper TFAWS06-1008, The 17th Thermal and Fluids Analysis Workshop, University of Maryland, August 2006.

[13]Saunders, D., Yoon, S., Wright, M., "An Approach to Shock Envelope Grid Tailoring and Its Effect on Reentry Vehicle Solutions," AIAA-2007-207, Jan 2007.

[14]Laub, B., Chen, Y.-K., Dec, J., "Development of a High-Fidelity Thermal/Ablation Response Model for SLA-561V," AIAA 2009-4232, June 2009.

[15]Sepka, S., Wright, M., "A Monte Carlo Approach to FIAT Uncertainties — Improvements and Results for MSL," AIAA-2009-4234, June 2009.